



Supplementary Materials

Investigating Pervaporation as a Process Method for Concentrating Formic Acid Produced from Carbon Dioxide

Section S1. Pervaporation equipment and experimental data

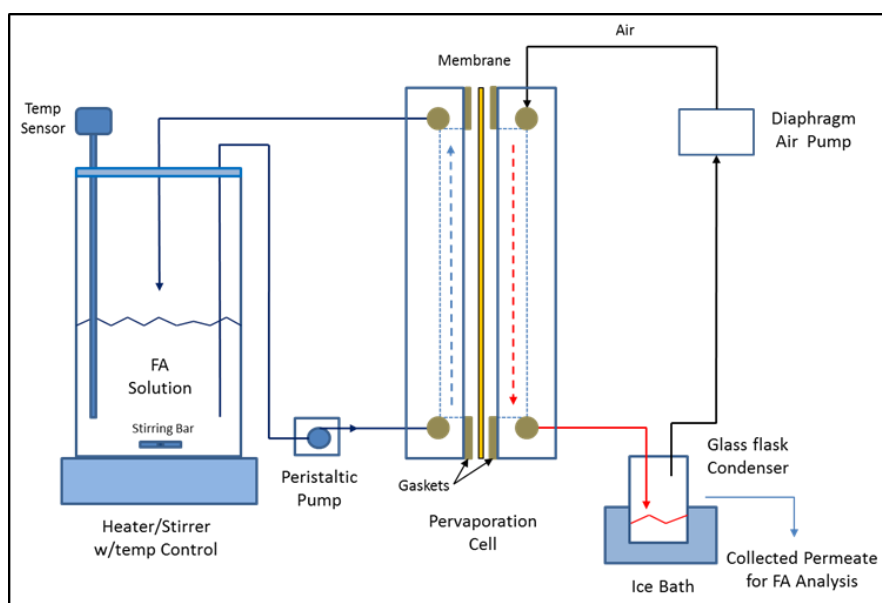


Figure S1. Experimental FA-H₂O pervaporation test system arrangement.

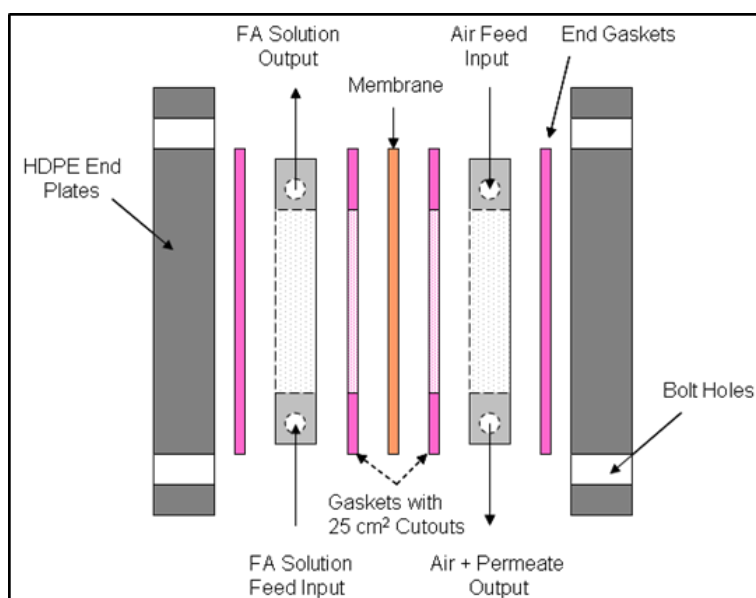


Figure S2. Experimental pervaporation cell configuration schematic - side view.



Figure S3. The 25 cm² pervaporation cell assembled outside view shown in (a). The pervaporation cell internal view is shown in (b), showing one of the membranes (Targray) being positioned in the cell for testing.

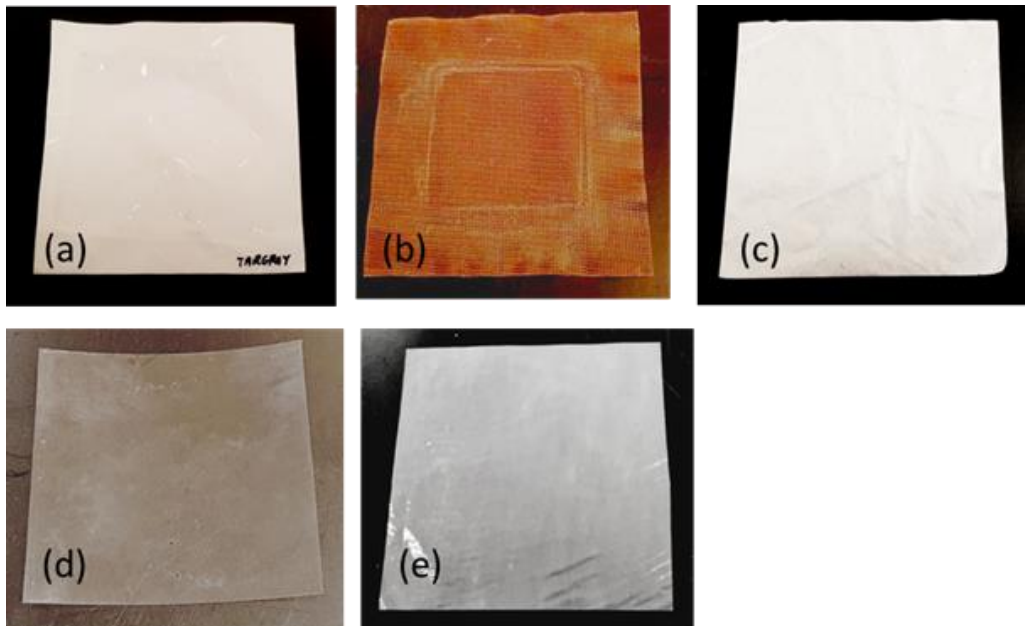


Figure S4. Photos of the various microporous and ion exchange membranes tabulated in Table 1. The membranes are: (a) Targray SD425101, (b) Nafion[®] N324, (c) Lydall Solupor[®] 4PO4A, (d) Sustainion[®] 37-50 anion exchange membrane, and (e) Sustainion[®] 37-50 T ePTFE reinforced anion exchange membrane.

Table S1. Summary table of all the pervaporation experimental data.

Membrane	Temp	Collection Time	Feed Composition (wt%)		Permeate Composition (wt%)		Permeability Separation Factor	Total Permeate Collected	Permeate Composition Collected		Permeation Flux or Rate of Water and FA through Membrane		H ₂ O/FA Flux Ratio		
			H ₂ O (A)	FA (B)	H ₂ O (A)	FA (B)			H ₂ O (g)	FA (g)	kg/m ² ·h	kg/m ² ·h			
Nafion® 324	22	24.00	90.78	9.22	96.36	3.64	2.69	14.91	14.37	0.54	H ₂ O	0.239	FA	0.009	26.5
Nafion® 324	40	24.00	90.77	9.23	96.74	3.26	3.02	28.71	27.77	0.94	H ₂ O	0.463	FA	0.016	29.7
Nafion® 324	60	24.00	88.31	11.69	96.9	3.10	4.14	44.51	43.13	1.38	H ₂ O	0.719	FA	0.023	31.3
Nafion® 324	60	3.25	79.85	20.15	91.75	8.25	2.81	5.10	4.68	0.42	H ₂ O	0.576	FA	0.052	11.1
Nafion® 324	60	2.17	70.02	29.98	86.42	13.58	2.72	3.55	3.07	0.48	H ₂ O	0.566	FA	0.089	6.4
Nafion® 324	60	3.83	59.85	40.15	79.39	20.61	2.58	6.98	5.54	1.44	H ₂ O	0.579	FA	0.150	3.9
Nafion® 324	60	3.33	40.6	59.4	65.44	34.56	2.77	3.51	2.30	1.21	H ₂ O	0.276	FA	0.146	1.9
Targray SD425101	22	24.00	89.07	10.93	95.86	4.14	2.84	13.45	12.89	0.56	H ₂ O	0.215	FA	0.009	23.2
Targray SD425101	40	24.00	89.73	10.27	96.14	3.86	2.85	50.02	48.09	1.93	H ₂ O	0.801	FA	0.032	24.9
Targray SD425101	60	5.00	89.9	10.10	95.49	4.51	2.38	7.22	6.89	0.33	H ₂ O	0.552	FA	0.026	21.2
Targray SD425101	60	5.00	80.22	19.78	93.62	6.38	3.62	8.50	7.96	0.54	H ₂ O	0.637	FA	0.043	14.7
Targray SD425101	60	5.00	65.2	34.8	83.98	16.02	2.80	8.50	7.14	1.36	H ₂ O	0.571	FA	0.109	5.2
Targray SD425101	60	3.00	39.9	60.1	54.88	45.12	1.83	5.45	2.99	2.46	H ₂ O	0.399	FA	0.328	1.2
Sustainion® 37-50 T ePTFE Reinforced	60	3.00	79.95	20.05	85.78	14.22	1.51	10.10	8.66	1.44	H ₂ O	1.155	FA	0.191	6.0
Sustainion®37-50 T ePTFE Reinforced	60	1.83	39.9	60.10	57.9	42.10	2.07	4.90	2.84	2.06	H ₂ O	0.620	FA	0.451	1.4
Lydall 4PO4A	60	1.25	79.95	20.05	90.3	9.70	2.33	1.30	1.17	0.13	H ₂ O	0.376	FA	0.040	9.3
Sustainion® 37-50	60	3.00	79.95	20.05	89.92	10.08	2.24	5.70	5.13	0.57	H ₂ O	0.683	FA	0.077	8.9
Sustainion® 37-50	60	3.50	90.06	9.94	93.37	6.63	1.55	6.98	6.52	0.46	H ₂ O	0.745	FA	0.053	14.1

Note: * Concentration A/B (wt%) in the permeate divided by the concentration A/B in the feed



Table S2. Batch permeation calculation for a starting 1 tonne 10 wt% FA feed solution using a 100 m² Targray membrane area pervaporation cell module, and operation for a 9.5 hour period at a temperature of about 40°C to produce a 32.1 wt% FA product concentration.

Constant Flux Rate kg/m ² h		Time Increment in h	Feed Mass in kg		Feed Composition FA wt%	Permeate Mass Change in kg per time interval		Cumulative Permeate Mass in kg		Permeate Composition FA wt%
FA	H ₂ O		FA	H ₂ O		FA	H ₂ O	FA	H ₂ O	
0.026	0.78	0.0	100.0	900	10.0	0.00	0.0	0.0	0	3.23
		0.5	98.7	861.0	10.3	1.30	39.0	1.3	39.0	3.23
Membrane Area		1.0	97.4	822.0	10.6	1.30	39.0	2.6	78.0	3.23
100 m²		1.5	96.1	783.0	10.9	1.30	39.0	3.9	117.0	3.23
		2.0	94.8	744.0	11.3	1.30	39.0	5.2	156.0	3.23
Temp: 40°C		2.5	93.5	705.0	11.7	1.30	39.0	6.5	195.0	3.23
		3.0	92.2	666.0	12.2	1.30	39.0	7.8	234.0	3.23
		3.5	90.9	627.0	12.7	1.30	39.0	9.1	273.0	3.23
		4.0	89.6	588.0	13.2	1.30	39.0	10.4	312.0	3.23
		4.5	88.3	549.0	13.9	1.30	39.0	11.7	351.0	3.23
		5.0	87.0	510.0	14.6	1.30	39.0	13.0	390.0	3.23
		5.5	85.7	471.0	15.4	1.30	39.0	14.3	429.0	3.23
		6.0	84.4	432.0	16.3	1.30	39.0	15.6	468.0	3.23
		6.5	83.1	393.0	17.5	1.30	39.0	16.9	507.0	3.23
		7.0	81.8	354.0	18.8	1.30	39.0	18.2	546.0	3.23
		7.5	80.5	315.0	20.4	1.30	39.0	19.5	585.0	3.23
		8.0	79.2	276.0	22.3	1.30	39.0	20.8	624.0	3.23
		8.5	77.9	237.0	24.7	1.30	39.0	22.1	663.0	3.23
		9.0	76.6	198.0	27.9	1.30	39.0	23.4	702.0	3.23
		9.5	75.3	159.0	32.1	1.30	39.0	24.7	741.0	3.23

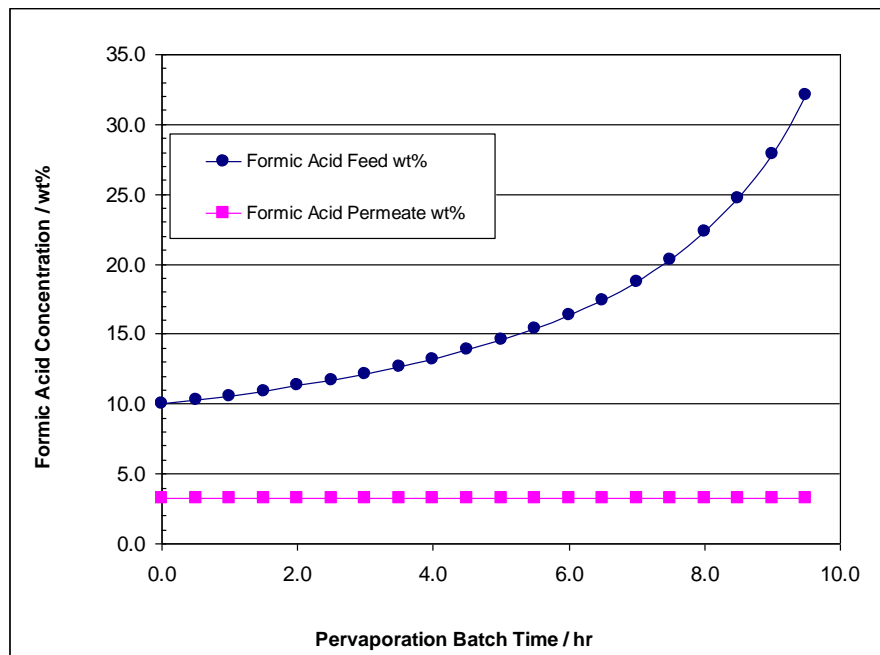


Figure S5. Theoretical calculated concentration change in the FA feed solution and permeate in a batch permeation run starting with a 10 wt% FA feed solution. Assumptions were for a 100 m² permeation membrane area stack, operation for a 9.5 hour period at a temperature of about 40°C, and constant permeation mass flux rates of water and FA of 0.78 kg/m²·h and 0.028 kg/m²·h respectively.

Section S2. Azeotropic distillation and CHEMCAD 6.01 azeotropic distillation simulation runs

S2.1 Azeotropic distillation and CHEMCAD 6.01 azeotropic distillation simulation runs

Formic acid -water solutions have a temperature- maximum azeotropic composition with a composition of 77.5 wt% formic acid (0.56 mole fraction FA) with a boiling point of 107.3°C at 101.325 kPa (1 atm) absolute pressure. Formic acid-water solutions also have a pressure-minimum azeotropic composition of 54.6 wt% FA (0.32 mole fraction FA) at an absolute pressure of 2.75 kPa (0.0271 atm).

Figure S6 shows a schematic of one simplified system configuration where the formic acid product output from the electrochemical reduction of CO₂ to formic acid electrolyzer is used as a feed to an azeotropic pressure distillation unit to produce commercial concentrations of formic acid of 80% or greater [1-4].

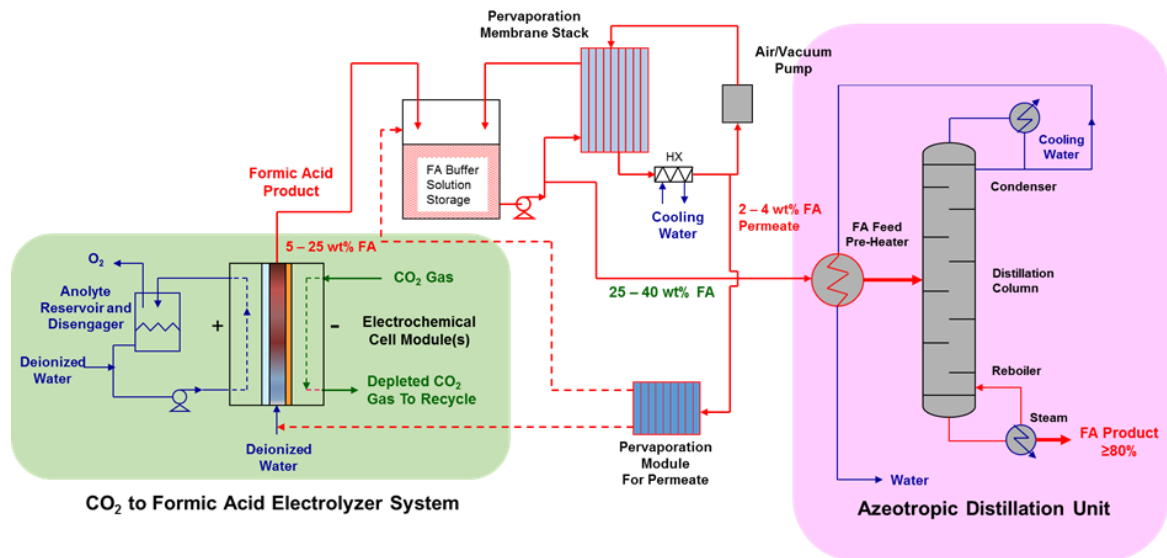


Figure S6. Conceptual system using the electrochemical FA cell integrated with pervaporation units and a single high pressure azeotropic distillation unit to produce commercial concentrations of FA.

Table S3. shows the azeotropic formic acid-water composition and boiling points as a function of pressure tabulated from reference [5]. Some of the issues with operating an azeotropic distillation at the higher pressures, where the right materials of construction have to be utilized and the impact of higher formic acid decomposition losses at operating at higher temperatures.

Table S3. Azeotropic formic acid-water composition and boiling point (BP) as a function of pressure (in bar) from reference [5].

Pressure bar	BP of Azeotropic Mixture °C	Formic Acid Content wt%
0.093	48.6	66.2
0.267	72.3	70.5
1.013	107.6	77.6
2.026	128.7	84
3.140	144	85

S2.2 Azeotropic Distillation Simulation Runs Using CHEMCAD 6.01

Azeotropic distillation simulation runs were conducted using a CHEMCAD version 6.01 chemical process simulation software (Chemstations, Inc., Houston, TX). Figures S7 – S9 show the simulation azeotropic runs conducted at pressures of 110, 220.6, and 330.9 kPa with the feed stream having an FA concentration of 20 wt% FA and showing the overhead and bottoms final product concentration results. The simulations used the NRTL model for the thermodynamic data and internal data sets. Figure S10 shows the simulation at a pressure of 330.9 kPa employing a heat exchanger on the overhead water product stream to preheat the FA solution feed. A second heat exchanger on the FA product bottoms was not added in this simulation.

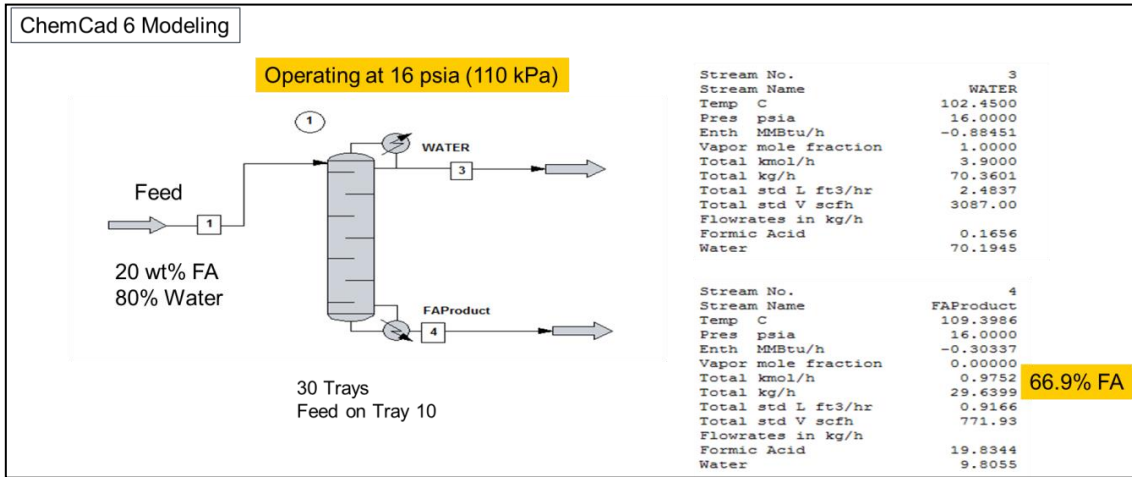


Figure S7. CHEMCAD 6.01 azeotropic distillation simulation modeling of the FA-water system at a pressure of 110 kPa maximizing the formic acid product concentration and minimizing FA in the overhead water product. The FA product output stream was 66.9 wt% at these conditions, not reaching the expected 77.5 wt% at these simulation conditions.

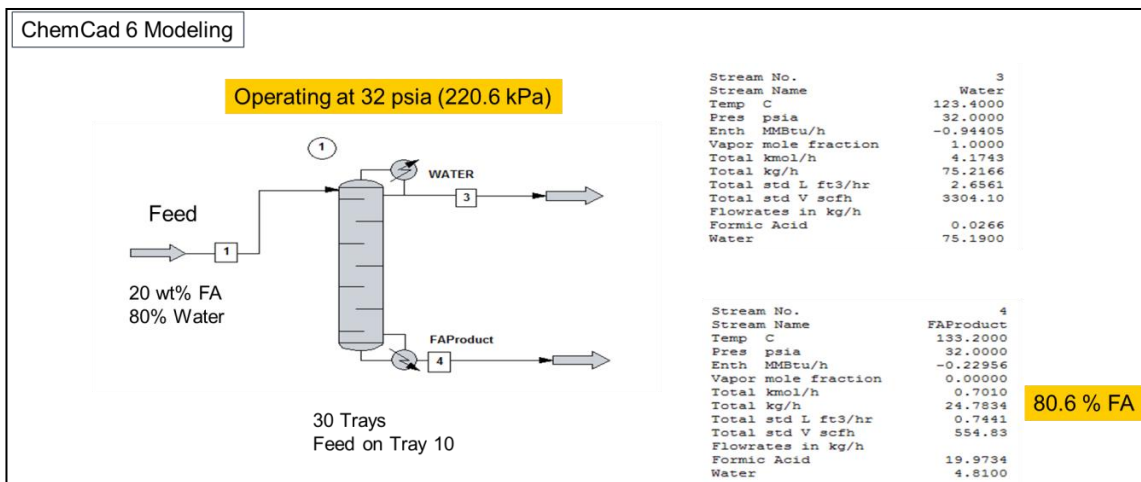


Figure S8. CHEMCAD 6.01 azeotropic distillation simulation modeling of the FA-water system at a pressure of 220.6 kPa maximizing the formic acid product concentration and minimizing FA in the overhead water product. The FA product output stream was 80.6 wt% at these conditions.

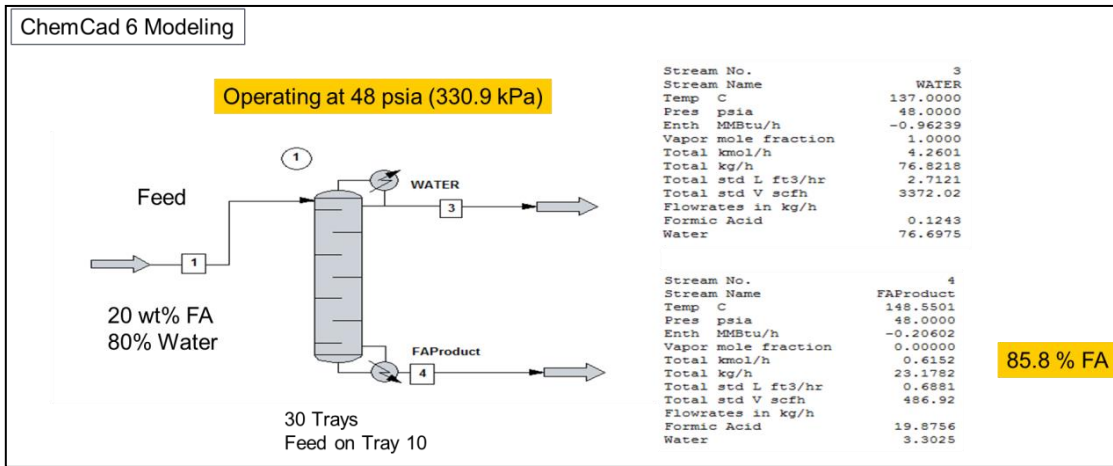


Figure S9. CHEMCAD 6.01 azeotropic distillation simulation modeling of the FA-water system at a pressure of 330.9 kPa maximizing the formic acid product concentration and minimizing FA in the overhead water product. The FA product output stream was 85.8 wt% at these conditions.

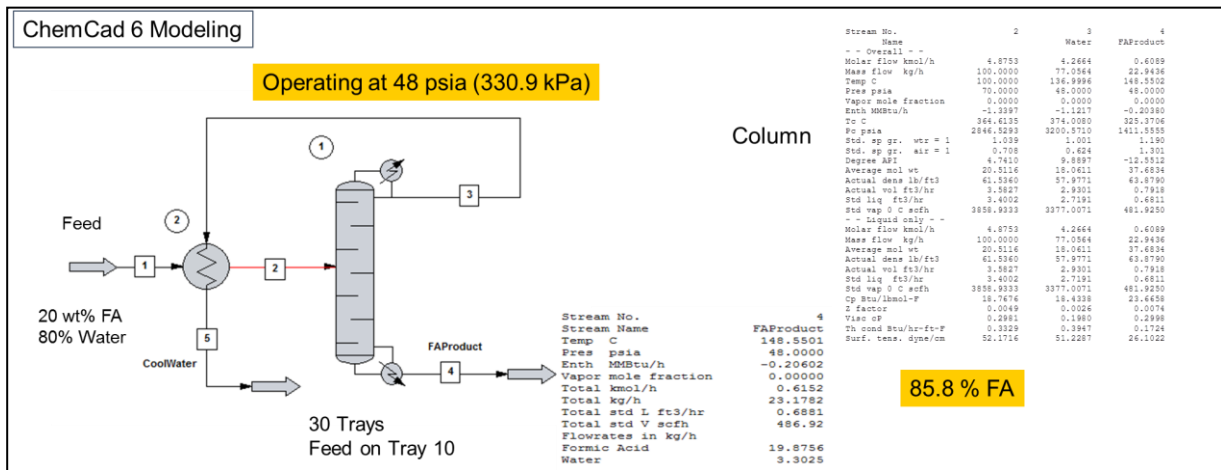


Figure S10. ChemCad 6.01 azeotropic distillation simulation modeling of the FA-water system at a pressure of 330.9 kPa maximizing the formic acid product concentration and minimizing FA in the overhead water product. The modeling had the addition of a heat exchanger to preheat the FA solution feed from the overhead water product stream.

Table S4. Summary of the Azeotropic distillation simulation column overhead and bottoms FA and H₂O wt% composition.

Column Section	Azeotropic Distillation Column Operating Pressure					
	110 kPa		220.6 kPa		330.9 kPa	
	FA wt%	H ₂ O wt%	FA wt%	H ₂ O wt%	FA wt%	H ₂ O wt%
Column Overheads Composition	0.24	99.76	0.04	99.96	0.16	99.84
Column Bottoms Composition	66.92	33.08	80.59	19.41	85.75	14.25

Section S3. Generated NRTL ChemCad VLE data for formic acid/water at various constant temperatures

ChemCad was used to generate the formic acid-water Txy equilibrium plots at various constant temperatures. The data shows how the azeotropic composition shifts to a higher FA concentration with increasing temperature.

- Figures S11 and S12 show the Txy calculated results at a constant temperature of 22 °C
- Figures S13 and S14 show the Txy calculated results at a constant temperature of 40 °C
- Figures S15 and S16 show the Txy calculated results at a constant temperature of 60 °C
- Figures S17 and S18 show the Txy calculated results at a constant temperature of 80 °C
- Figures S19 and S20 show the Txy calculated results at a constant temperature of 100 °C

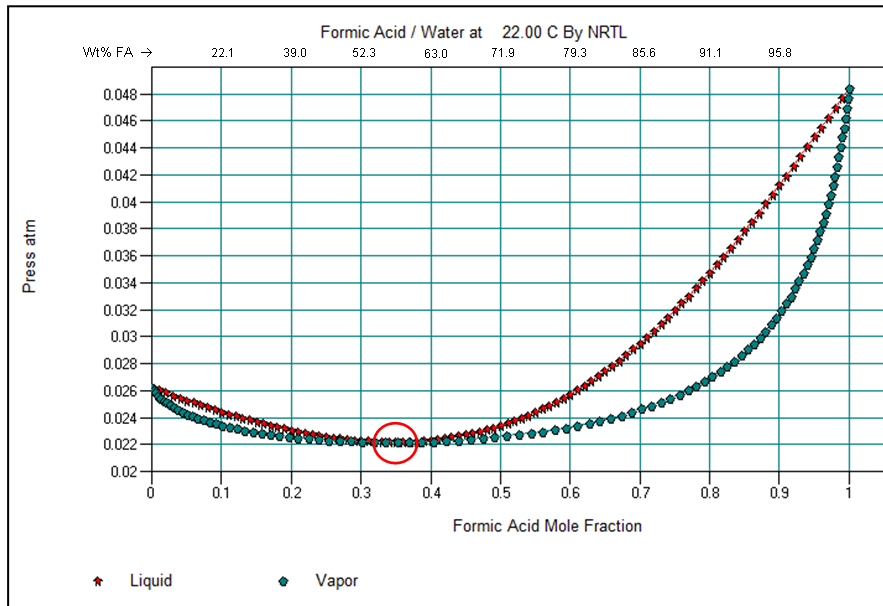


Figure S11. Formic acid-water Txy vapor equilibrium plot at a constant temperature of 22°C generated using ChemCad generated NRTL data. The circle shows the pressure-minimum azeotrope composition.

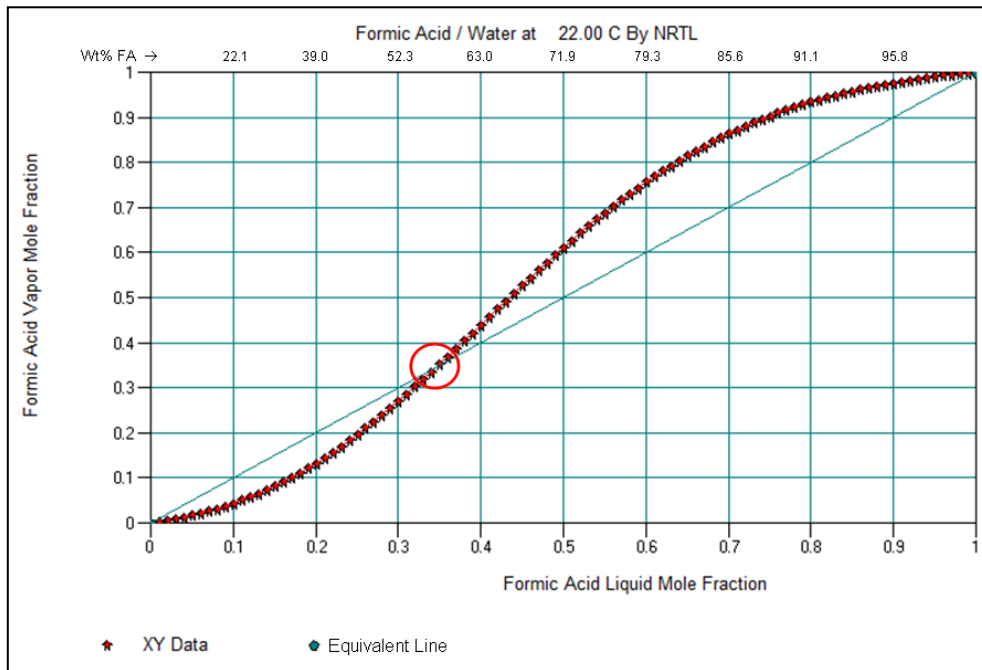


Figure S12. Formic acid-water Txy vapor equilibrium plot at a constant temperature of 22°C generated using ChemCad generated NRTL data. The circle shows the azeotrope composition at that temperature.

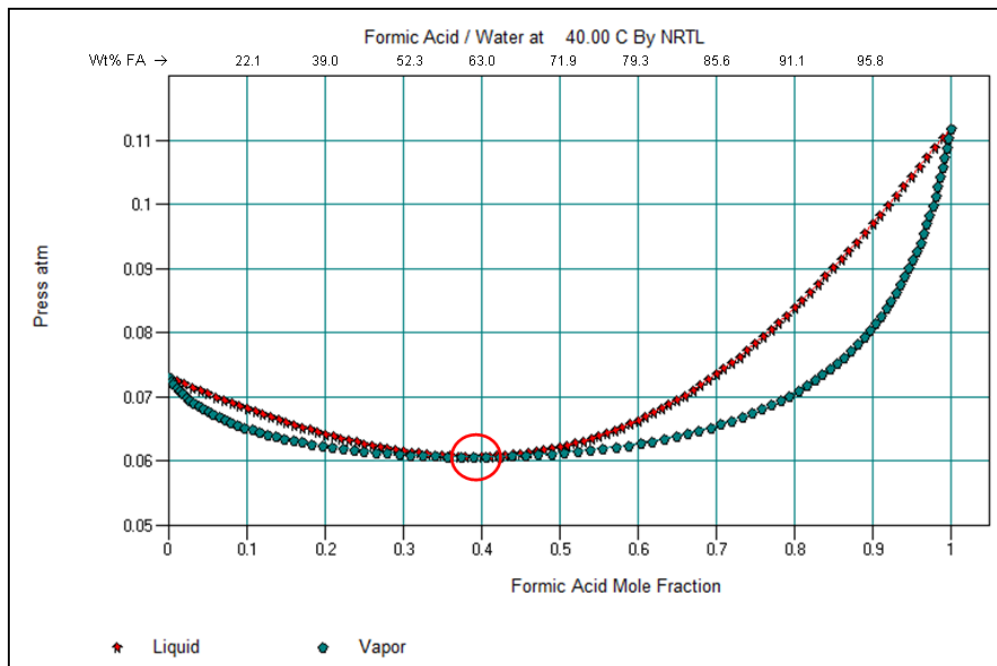


Figure S13. Formic acid-water vapor Txy equilibrium plot at a constant temperature of 40°C generated using ChemCad generated NRTL data. The circle shows the pressure-minimum azeotrope composition.

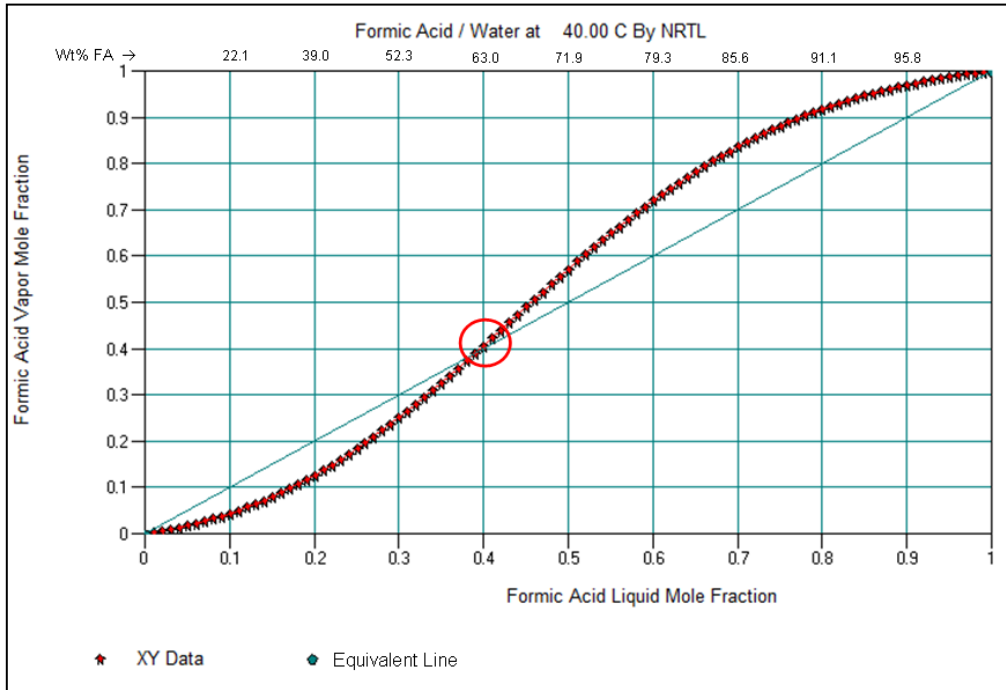


Figure S14. Formic acid-water vapor Txy equilibrium plot at a constant temperature of 40°C generated using ChemCad generated NRTL data. The circle shows the azeotrope composition at those conditions.

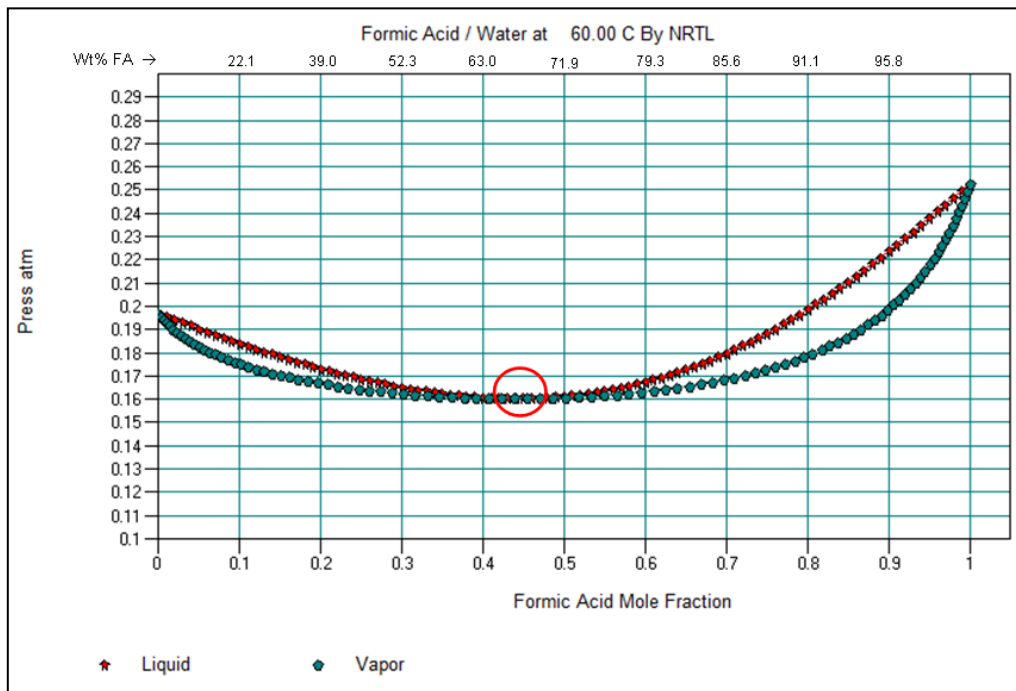


Figure S15. Formic acid-water Txy vapor equilibrium plot at a constant temperature of 60°C generated using ChemCad generated NRTL data. The circle shows the pressure-minimum azeotrope composition.

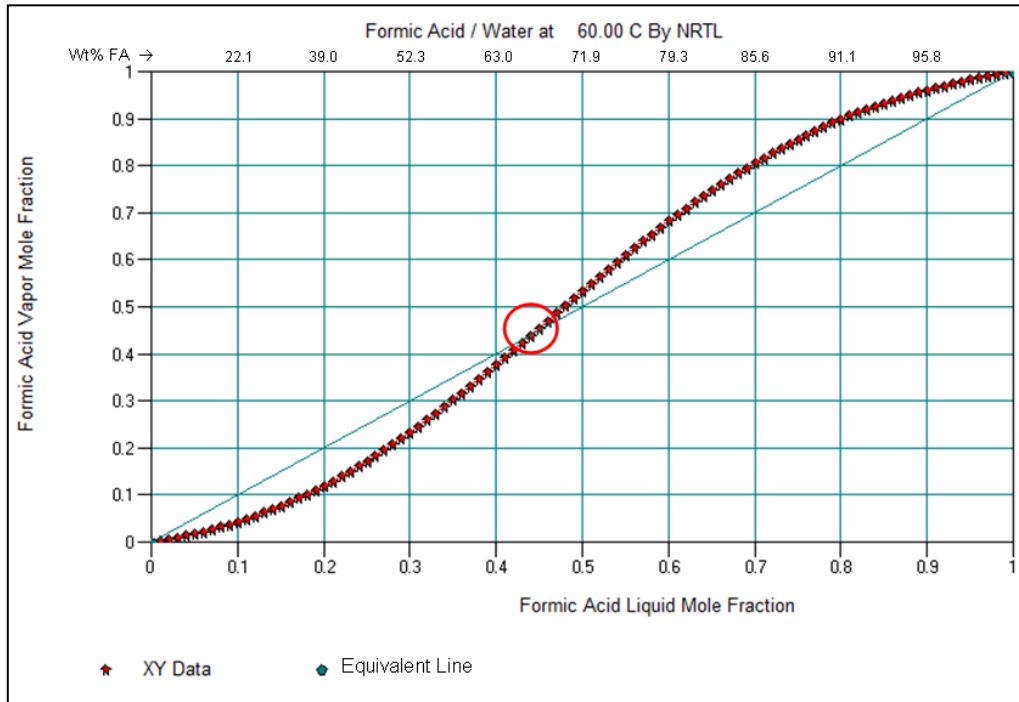


Figure S16. Formic acid-water Txy vapor equilibrium plot at a constant temperature of 60°C generated using ChemCad generated NRTL data. The circle shows the azeotrope composition at those conditions.

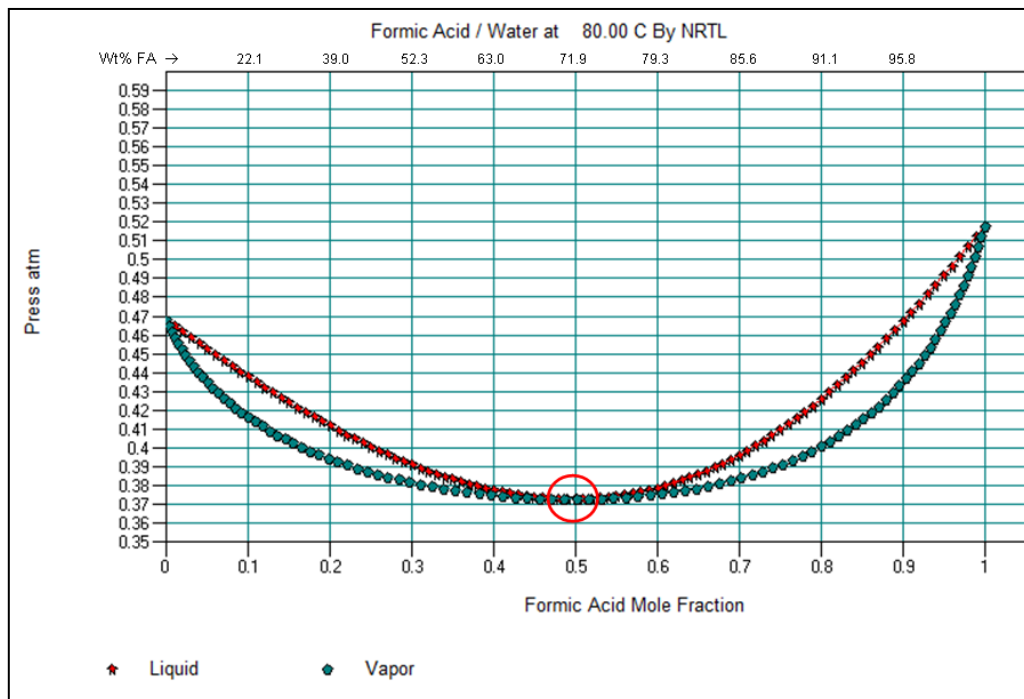


Figure S17. Formic acid-water Txy vapor equilibrium plot at a constant temperature of 80°C generated using ChemCad generated NRTL data. The circle shows the pressure-minimum azeotrope composition.

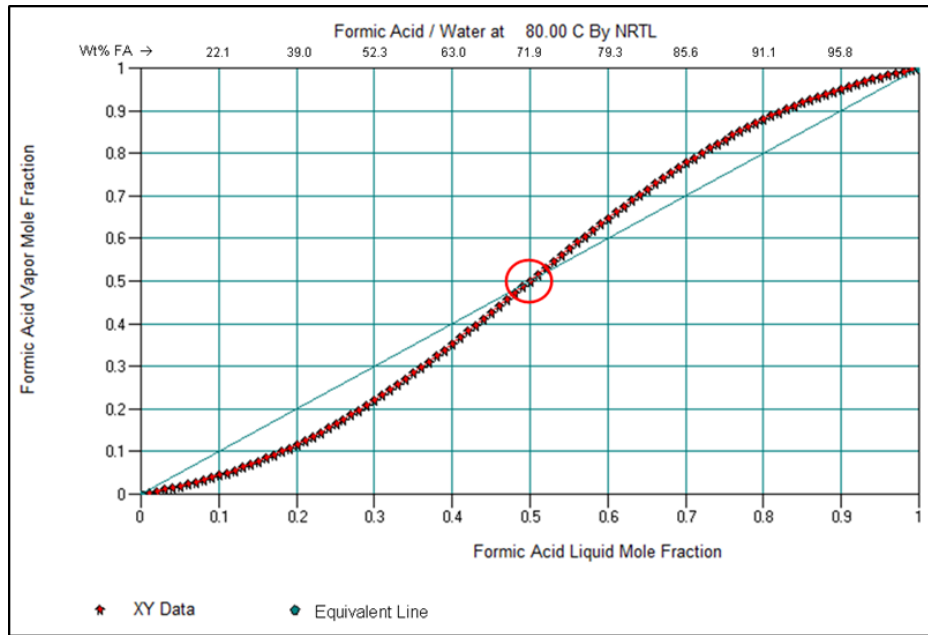


Figure S18. Formic acid-water Txy vapor equilibrium plot at a constant temperature of 80°C generated using ChemCad generated NRTL data. The circle shows the azeotrope composition at those conditions.

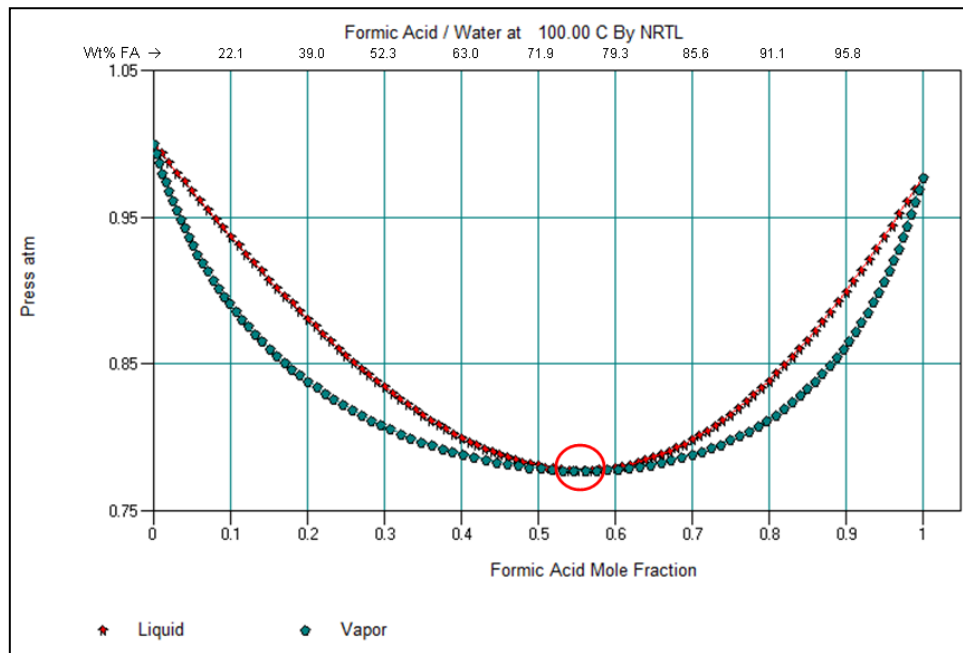


Figure S19. Formic acid-water vapor Txy equilibrium plot at a constant temperature of 100°C generated using ChemCad generated NRTL data. The circle shows the pressure-minimum azeotrope composition.

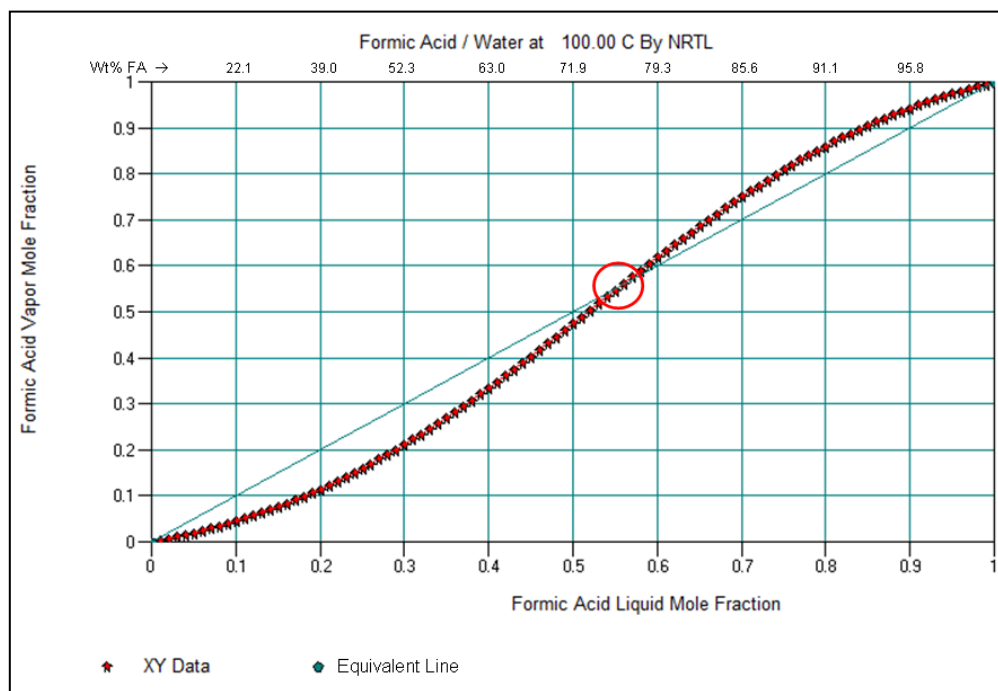


Figure S20. Formic acid-water Txy vapor equilibrium plot at a constant temperature of 100°C generated using ChemCad generated NRTL data. The circle shows the azeotrope composition at those conditions.

Section S4. References

1. Yang, H.; Kaczur, J. J.; Sajjad, S. D.; Masel, R. I., Electrochemical conversion of CO₂ to formic acid utilizing Sustainion™ membranes. *Journal of CO₂ Utilization* **2017**, *20*, 208-217.
2. Yang, H.; Kaczur, J. J.; Sajjad, S. D.; Masel, R. I., CO₂ Conversion to Formic Acid in a Three Compartment Cell with Sustainion™ Membranes. *ECS Transactions* **2017**, *77* (11), 1425-1431.
3. Kaczur, J. J.; Yang, H.; Sajjad, S. D.; Masel, R. I. Method and system for electrochemical production of formic acid from carbon dioxide. U.S. Patent 10,047,446 (**2018**).
4. Kaczur, J. J.; Yang, H.; Sajjad, S. D.; Masel, R. I. In (437f) *Modeling Methods for Concentrating a Formic Acid Product Generated from a Novel Electrochemical Reduction of CO₂ Cell Design* AIChE 17th Annual Conference, Minneapolis, MN, Minneapolis, MN, **2017**.
5. Hietala, J.; Vuori, A.; Johnsson, P.; Pollari, I.; Reutemann, W.; Kieczka, H., Formic Acid. In *Ullmann's Encyclopedia of Industrial Chemistry*, **2016**; pp 1-22.